12^{th} International Conference on Fracture Mechanics of Concrete and Concrete Structures
FraMCoS-12
B.L.A. Pichler, Ch. Hellmich, P. Preinstorfer (Eds)

https://doi.org/10.21012/FC12.1384
TT-C1:1

SMEARED CRACKING AND DISCRETE CRACK DILATANCY APPLIED TO TENSION-SHEAR MODEL PROBLEMS

NIELS W. KOSTENSE*, YUGUANG YANG*, MAX A.N. HENDRIKS*† AND JAN G. ROTS*

* Delft University of Technology, Faculty of Civil Engineering and Geosciences,
Stevinweg 1, 2628 CN Delft, The Netherlands
e-mail:

†Norwegian University of Science and Technology
Trondheim, Norway

Key words: Smeared crack models, Crack dilatancy, Tension shear, Finite element analysis

Abstract. In this paper, the performance of smeared crack and discrete crack dilatancy models applied to mixed mode fracture is evaluated. Fixed, rotating as well as hybrid rotating-to-fixed smeared crack models are considered. For each crack model format-specific input parameters such as the shear retention factor, the reduction of compressive strength due to lateral cracking, and the transition point from rotating to fixed are varied respectively. Elementary tension-shear model problems are considered including validation against recent mixed-mode lab tests. The results indicate that the fixed crack response is highly sensitive to the choice of shear retention factor, while the rotating crack results are sensitive to the adopted boundary conditions of the model problem. The hybrid crack formulation does not provide consistent advantages compared to the fixed or rotating crack formulations. The discrete crack dilatancy models are found to be more accurate in predicting the mixed mode response of the tests, although they tend to overestimate the shear strength. Reference is made to early work by Willam.

1 INTRODUCTION

In the field of civil engineering, the employment of non-linear finite element analysis (NLFEA) is becoming an increasingly popular approach for the strength assessment of concrete structures. The detailed insight into the structural behaviour that can be obtained by NLFEA has shown its great potential, and guidelines [1] have been established to decrease the model uncertainty and promote a uniform modelling approach. In performing such analyses, the smeared crack models based on the total strain concept [2] are frequently adopted. The total strain based crack model has proven its advantages in terms of accuracy and robustness, while the intuitive input in terms of direct engineering stress-strain relations are appreciated by practicing engineers.

Within the total strain-based smeared crack framework, various choices are left to the user. The crack orientation is the most fundamental one, where a fixed, rotating, or rotating-to-fixed format can be specified. In the fixed formulation, the crack plane direction remains fixed after crack initiation. This allows the principal strain direction to deviate from the crack plane direction. Consequently, shear stresses on the crack plane can develop and can, to a certain extent, be handled by a shear retention factor, which is a scalar variable reducing the shear stiffness on the crack plane. Common practice in the early days was to adopt a constant shear

retention factor, with typical values in the range of $\beta_s = [0.01 - 0.1]$. Such constant shear retention factor may result in shear stresses on the crack plane that increase excessively. This potentially leads to an overprediction of the resistance, specifically in the case of shear-critical reinforced concrete beams without shear reinforcement. An alternative and more realistic approach is to use a variable shear retention factor that decreases with increasing mode-I crack normal strain. Early fixed smeared crack models with incremental decomposed strain formulations appeared to be sensitive to stress locking. This stimulated the development of Rotating crack models. Rotating crack models describe the stress-strain relations in the continuously rotating principal strain directions. These are considered to be more robust and were supposed to provide a lower bound capacity as no excessive shear build-up along fixed cracks could happen. Nevertheless, rotating crack formulations may suffer from so-called overrotation. For RC structures this could trigger delamination of the boundary elements [3] and potentially give an unrealistic direct load transfer to the supports [4]. The latter tends to overpredict the resistance as well.

An alternative to the fixed or rotating formulation is provided by the multi-directional fixed crack model [5] in an incremental and decomposed strain format. Furthermore, hybrid rotating-to-fixed crack models have been proposed, which transition from rotating to fixed once a specified condition is met. From a phenomenological point of view, the rotating-to-fixed crack formulation seams appealing as it reflects the fracture process. The tension softening is characterized by progressive microcracking, and once these microcracks evolve, they coalesce to form a macro crack. Up to the point where the microcracks coalesce, the direction of the major crack is not fixed and allows for rotation by changing the strain state, hence supporting the transition from a rotating to a fixed crack formulation. For the mutual comparison between the different smeared crack formulations often the well-known strain-driven tension-shear model problem proposed by Willam et al. [6] is adopted. Further insights can be gained by not only mutually comparing numerical modelling results but also by validating them against experimental data. In this study, the mixed mode fracture experimental campaign conducted by Jacobsen et al. [7] is used for such validation. This experiment distinguishes itself from preceding studies in mixed-mode fracture and aggregate interlock by combining two key aspects: (1) first creating a partial mode-I crack driven by pure tension, followed by (2) a certain mixed-mode tension-shear straining. These tests allow the models to be validated against experimental data, in similar fashion as the single element tension-shear problem. Inspired by the work of Willam [6], Rots [8], and Feenstra [9], various smeared crack models are evaluated by means of strain-driven single element tests and compared with experimental data.

2 METHODS

2.1 Mixed mode crack experiments

To study the performance of various modeling approaches in describing mixed-mode fracture behavior, the experimental campaign conducted by Jacobsen et al. [7] is taken as a reference. The experiment investigates the mixed-mode crack development behavior of concrete using a biaxial testing machine designed to apply normal and shear loads simultaneously, as illustrated in fig. 1.

The test setup comprises a very stiff testing frame and support structure, enabling precise control of displacements in two perpendicular directions. The test specimens are double-notched concrete blocks with dimensions of 150 mm in width, 80 mm in height, and 75 mm in depth, with notches of 55 mm depth creating a ligament area of 40×75 mm^2. The concrete, with a minimum and maximum aggregate size of 4 mm and 8 mm respectively, has an anticipated 28-day strength of $f_c = 30.$ MPa and reported material properties of tensile strength $f_t = 3.3$ MPa, elastic modulus $E_c = 31$ GPa, and fracture energy in the range

$G_f = [115 - 165]$ N/m.

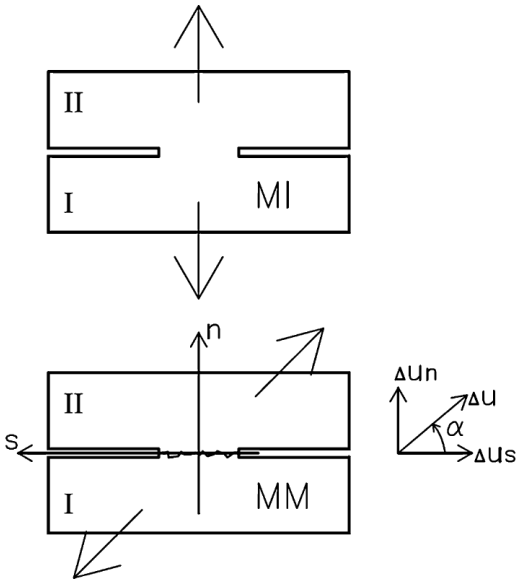

Figure 1: Loading scheme: Mode I opening phase (top) and mixed-mode phase (bottom) of the experiment by Jacobsen et al. [7]

The experimental loading procedure consists of two phases. An initial pure Mode I prescribed displacement $\Delta U_n = U_{n0}$ is applied to initiate a crack (Phase 1), followed by a mixed-mode phase to analyze the interaction between normal (ΔU_n) and shear (ΔU_s) displacements (Phase 2). Crack initiation occurs in pure Mode I, while the mixed-mode opening angle (α) defines the relative displacement direction $\tan(\alpha) = \Delta U_n / \Delta U_s$. Several loading scenarios are applied to the specimens, with varying initial Mode I openings (U_{n0}) from 0.015 mm to 0.100 mm and mixed-mode angles α from $40°$ to $60°$. Note that the crack widths initiated in the Mode I loading phase are still within the tension-softening regime of the concrete. Clip gauges mounted on orthogonal rails measure displacements between the cracked segments.

In particular, the relations between normal stress and crack opening displacement, as well as between shear stress and sliding displacement, are of interest. Although multiple experiments with various loading conditions have been conducted, the focus of this study is on the models with $U_{n0} = 0.04$ mm and $\alpha = 45°$.

2.2 Smeared crack approach

The numerical models reflect the experimental setup with material properties provided by Jacobsen et al. [7]. To simplify the analysis, the models assume a homogeneous stress and strain state, reducing the problem to a single element subjected to imposed normal and shear displacements. The model is defined by a single two-dimensional 4-noded quadrilateral plane stress element. Under the assumption that the uncracked part of the specimen has a negligible influence on the fracture process, a square element with the size of 40×40 mm^2 is modeled. With a thickness of 75 mm, the resulting ligament area is identical to the experimental specimens. A standard 2×2 Gauss integration scheme is adopted, and the loading is applied in the same manner as in the experiments. First, a prescribed displacement-controlled load is applied to the upper nodes, followed by simultaneous and equal normal and shear displacements. The models are subjected to the same loading conditions as the experiments, focusing on the mixed-mode phase with $U_{n0} = 0.04$ mm and $\alpha = 45°$. The material properties defined in the numerical models are presented in table 1, and the numerical models are illustrated in fig. 2.

Table 1: Adopted concrete properties in numerical models

Property	Value	Unit
E_{c}	31000	N/mm^2
ν	0.22	-
f_{c}	41	N/mm^2
f_{t}	3.3	N/mm^2
G_{t}	0.14	N/mm
G_{C}	35	N/mm
D_{min}	4	mm
D_{max}	8	mm
h_{cr}	40	mm

In the smeared crack models, the total-strain based crack model is used (Feenstra et al. [2]). A full description goes beyond the scope of this paper; however, the most important features

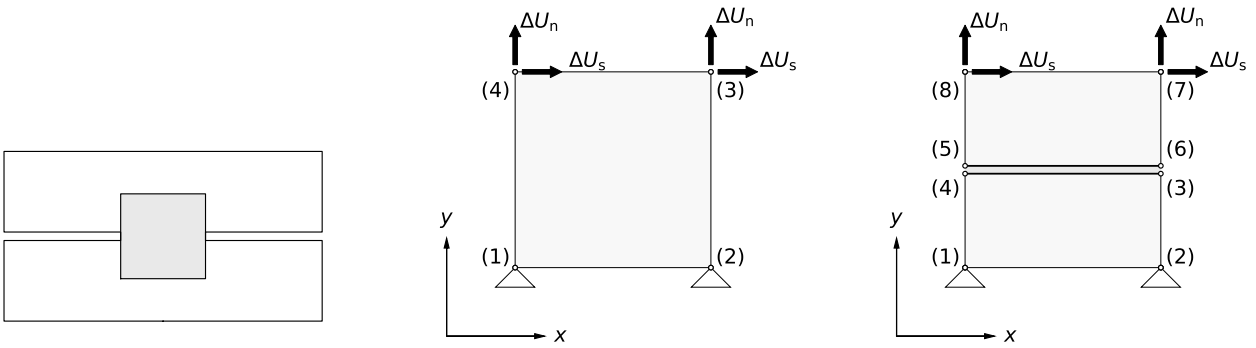

(a) Specimen area represented by numerical model

(b) Smeared crack

(c) Crack dilatancy

Figure 2: Modeling approach

are highlighted. For the purpose of the present study, the existing models available in the Finite Element code DIANA are employed, allowing for *fixed*, *rotating*, and *rotating-to-fixed* crack formulations. The model accounts for the cracking and crushing behavior of concrete as well as interaction behavior. It presumes that incipient cracking occurs perpendicular to the direction of maximum principal strain, as illustrated in fig. 3a. After crack initiation, the crack n, t-coordinate system is introduced. Tension softening is characterized by a fracture energy G_f based curve adjusted by the crack bandwidth h_{cr}, following the crack band theory [10]. Specifically, an exponential softening curve proposed by Hordijk [11] is used. Similarly, in the compression regime, a parabolic stress-strain relation is employed following the work of Feenstra [12], as illustrated in fig. 3c. Reduction of the compressive strength due to lateral cracking is taken into account according to Vecchio et al. [13], defined by a reduction factor β_{c}. Additionally, the reduction can be limited by defining a minimum value of $\beta_{\mathrm{c}}^{\mathrm{min}}$. No increase in compressive strength due to confinement is considered. To establish a consistent comparison between different models, a predefined crack band estimator equal to the element size of 40mm is used instead of more advanced projection methods [14]. In this study, the crack direction format is varied between fixed, rotating, or rotating-to-fixed. Based on the adopted crack direction formulation, several options become available, and choices are discussed below.

Fixed crack format

A fundamental aspect of the fixed crack formulation is the way shear resistance on the crack plane is accounted for. A common approach is to introduce a shear retention factor β_{s}, which reduces the shear stiffness term in the constitutive model. This factor mimics the transfer of shear stresses across the crack plane due to aggregate interlock by:

$$G^{\mathrm{cr}} = \beta_{\mathrm{s}} G_{\mathrm{c}} \tag{1}$$

where G^{cr} is the shear stiffness on the crack plane and G_{c} is the initial elastic shear stiffness of uncracked concrete. The most straightforward implementation is achieved by defining a constant shear retention factor, typically in the range of $\beta_{\mathrm{s}} = [0.01 - 0.1]$. A more physically representative method involves a shear retention factor that decreases as the material damage accumulates [16]. Such a model is proposed by e.g. Al-Mahaidi [17], where the shear retention factor decreases as a function of the total strain normal to the crack:

$$\beta_{\mathrm{s}} = 0.4 \frac{f_{\mathrm{t}}}{E_{\mathrm{c}} \varepsilon_{nn}} \tag{2}$$

where f_{t} is the tensile strength of the concrete, E_{c} is the Young's modulus, and ε_{nn} is the

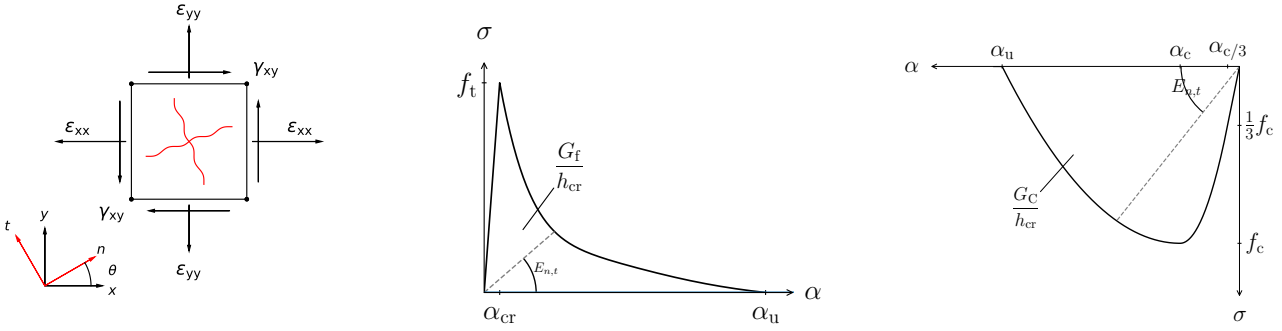

(a) Crack coordinate system **(b)** Tension softening [11] **(c)** Compression softening [15]

Figure 3: Total strain based smeared crack model

total strain normal to the crack plane.

An alternative approach is to use a so-called damage-based shear retention factor, being a function of the damage parameter, typically denoted as ω. In this way, the shear retention factor is reduced proportionally to the tensile softening, with the shear stiffness being reduced to zero when the damage parameter reaches unity, i.e., when the ultimate crack strain is reached at the end of the tension-softening regime. As a third option, an aggregate size-dependent shear retention factor based on the crack normal strain is defined as:

$$\beta_{\mathrm{s}} = 1 - \left(\frac{2\varepsilon_{\mathrm{nn}}^{\mathrm{cr}} h_{\mathrm{cr}}}{d_{\mathrm{agg}}} \right) \qquad (0 \leq \beta_{\mathrm{s}} \leq 1) \quad (3)$$

where d_{agg} is the mean aggregate size, $\varepsilon_{\mathrm{nn}}^{\mathrm{cr}}$ is the crack normal strain, and h_{cr} is the crack band width.

In this study, the fixed crack formulation is evaluated using the described shear retention factors: a set of constant shear retention factor of $\beta_{\mathrm{s}} = 0.1$ and $\beta_{\mathrm{s}} = 0.01$, a damage-based shear retention factor, the Al-Mahaidi shear retention factor, and an aggregate interlock-based shear retention factor.

Rotating crack format

In the rotating crack formulation, the crack direction is allowed to rotate and is updated at each iteration to align with the direction of the maximum principal strain. In this formulation, there is no explicit shear retention factor, but an implicit shear term that provides coaxiality between principal stress and principal strain. This allows for a continuously rotating crack and is expected to provide a lower bound capacity since the critical shear crack angle can be adjusted throughout the analysis. However, in RC applications the rotating crack formulation may suffers from over-rotation, which can trigger delamination of a boundary of elements [3,4], leading to an unrealistic direct load transfer to the supports and potentially overpredicting the capacity. In this study, the rotating crack formulation is extended by a factor β_{c} that reduces the compressive strength due to lateral cracking as proposed by Vecchio et el. [13]. Various limitations to the reduction factor are defined with minimum values set to $\beta_{\mathrm{c}}^{\mathrm{min}} = [1.0, 0.6, 0.4, 0.0]$.

$$\beta_{\mathrm{c}} = \frac{1}{1 + K_c} \leq 1 \quad (4)$$

with

$$\beta_{\mathrm{c}}^{\mathrm{min}} \leq \beta_{\mathrm{c}} \leq 1 \quad (5)$$

$$K_{\mathrm{c}} = 0.27 \left(-\frac{\alpha_{\mathrm{lat}}}{\varepsilon_0} - 0.37 \right) \quad (6)$$

$$\varepsilon_0 = -\frac{f_{\mathrm{c}}}{E_{\mathrm{c}}} \quad (7)$$

where α_{lat} is the lateral strain, f_{c} is the compressive strength of the concrete, E_{c} is the Young's modulus of the concrete.

Rotating-to-fixed crack formulation

A combination of the fixed and rotating crack formulations is provided by the hybrid rotating-to-fixed crack model. This model transitions from rotating to fixed once a specified condition is violated. The additional input parameter characterizing the rotating-to-fixed crack model is the threshold value, which determines the transition point from rotating to fixed crack. This threshold value is often expressed in terms of accumulated damage at the integration point level, or more specifically, the ratio between the residual tensile strength after cracking and the initial tensile strength, $c_{\text{fix}} = \sigma_{nn}^{cr}/f_t$.

Due to the limited use of this rotating-to-fixed formulation in practice, there is little guidance in the literature regarding the choice of the threshold value. In the rotating crack model with transition to scalar damage proposed by Jirasek et al. [18], a threshold value of $\alpha_{\text{fix}} = 0.3$ is reported to provide good results for the selected benchmark problem. This value is motivated by the adopted bi-linear tension softening relation, where the transition point conveniently coincides with the change in slope of the bilinear softening curve. Cervenka et al. [19] reported a higher threshold value of $c_{\text{fix}} = 0.7$, although no background information is provided. One could argue that the transition point should have a physical meaning, such as the stage where microcracks coalesce into a macroscopic crack. In a similar experimental study to [7], Østergaard et al. observed that when the tension load decreases to 50–70% of the maximum tensile capacity, the initial crack band between the notches can be interpreted to coalesce into a macro crack [20].

In the current implementation of the adopted total strain formulation, the transition point is defined by the crack strain in the normal direction of the crack plane. This approach is mesh size dependent as the tension softening behavior is defined as a function of the fracture energy. In this specific case, a predefined and constant crack band width is used, meaning that the transition point is known a priori. It should be noted that the rotating-to-fixed crack model produces meaningful results only when the element is subjected to mixed-mode loading conditions before the transition point is reached. If this is not the case, the model behaves as a fixed crack model. Conversely, if the crack strain for transition from rotating to fixed is not reached during the analysis, the model behaves identically to the rotating crack model.

Table 2: Transition points in rotating-to-fixed crack formulation

Name	c_{fix}	$\sigma^{\text{cr}}_{\text{nn;fix}}$	$\varepsilon^{\text{cr}}_{\text{nn;fix}} 10^{-3}$
Fixed	1.0	3.30	0.0
Fixed 70 %	0.7	2.31	0.31
Fixed 50 %	0.5	1.65	0.61
Fixed 30 %	0.3	0.99	1.16
Fixed 0 %	0.0	0.0	5.54
Rotate	0.0	0.0	∞

2.3 Discrete crack approach

Although smeared crack models are strongly preferred in nonlinear finite element analysis (NLFEA) of reinforced concrete structures, a discrete crack approach is included for comparison. Various crack dilatancy models have been implemented into DIANA in combination with a tensile softening pre-stage (Feenstra et al. [21, 22]) and are used herein. The discrete crack models are defined in a similar manner as the smeared crack models, yet two quadrilateral elements are now connected by an interface element. This interface element represents the crack opening and sliding behavior and is defined by a traction-separation law.

$$\begin{cases} t_n &= f_n(\Delta u_n, \Delta u_t) \\ t_t &= f_t(\Delta u_n, \Delta u_t) \end{cases} \tag{8}$$

The crack dilatancy models follow the total deformation theory, where the interface tractions (t_n, t_s) are expressed as a function of the total relative displacements $(\Delta u_n, \Delta u_t)$ [23],

also shown in eq. (8). To describe the development stage of Mode I cracking, a fracture energy-based linear tension softening is employed. During this stage, it must be decided how the shear stresses are transferred across the crack plane, and two extreme options are available: 1) full shear stiffness is retained until the critical crack opening displacement is reached, or 2) the shear stiffness is omitted, allowing for no shear transfer. In either case, a discontinuity in the shear stress is observed when the critical crack opening displacement is reached. In this particular study, the shear stiffness is neglected in the Mode I crack opening phase. Once the crack has reached the critical crack opening displacement, the crack is assumed to be fully open, and the relations for the Mode II crack dilatancy aggregate-interlock models are applied.

In the context of finite element analysis using a discrete crack modeling approach, the tractions and relative displacements on a crack plane can be described using cohesive or interface elements. While numerous models exist, this study focuses on five representative crack dilatancy models implemented in Diana FEA [21, 22]. The formulations for crack dilatancy can be broadly classified into two categories: empirical crack models and physical crack models.

The first category, empirical crack models, includes the Rough Crack Model by Bažant and Gambarova [23], which conceptualizes the crack surface as a regular array of trapezoidal asperities, leading to shear stress dependence on the displacement ratio and asymptotic behavior for large displacement ratios. Another empirical model is the Rough Crack Model by Gambarova and Karakoç [24], which refines the previous model by incorporating constant confinement stress and aggregate size effects, providing an improved formulation of the normal traction-displacement relationship. Additionally, the Aggregate Interlock Relation by Walraven and Reinhardt [25] offers linear relations derived from experimental results, obtained by fitting shear stress and crack width data.

The second category, physical crack models, comprises the Two-Phase Model by Walraven [26], which treats concrete as a two-phase material with stiff spherical inclusions in a plastic matrix, accounting for aggregate distribution and contact areas to determine shear and normal stresses. Lastly, the Contact Density Model by Li et al. [27] assumes a crack plane consisting of variously inclined contact units, with contact forces computed using an elasto-perfectly plastic model, and considers the loss of contact area with increasing normal crack displacement. The material properties, boundary conditions, and prescribed displacements are identical to those used in the smeared crack models. For a more detailed description of the finite element implementation of the crack dilatancy models, the reader is referred to the work of Feentra et al. [21, 22].

3 RESULTS

3.1 Fixed crack formulation

Please note that the results reported in this chapter belong to the boundary conditions as shown in fig. 2, i.e. the horizontal strain $\varepsilon_{\mathrm{xx}}$ is confined to zero, while first the vertical strain $\varepsilon_{\mathrm{yy}}$ is incremented to some level complying with a partial mode-I crack, whereafter both $\varepsilon_{\mathrm{yy}}$ and γ_{xy} are incremented in some proportion. The results of the fixed crack models are compared for both the shear and normal direction, where the global stresses are plotted against the relative displacements. First, the results from the $\tau - \Delta U_s$ curves from fig. 4a are discussed. The fixed crack models that adopt a constant shear retention factor show a linear relationship between the shear stress and shear strain. The analysis with a constant shear retention factor of $\beta_{\mathrm{s}} = 0.1$ severely overestimates the shear stresses, although the secant stiffness at the point where the ultimate shear stiffness is reached and the corresponding displacement is reasonably in line with the experiments. This is not the case for the constant shear retention factor of $\beta_{\mathrm{s}} = 0.01$, which significantly underestimates the shear stresses at smaller displacements. At higher displacement levels, the shear

stresses are again overestimated. Similar behavior is observed for the crack strain-dependent shear retention factor according to eq. (2), although the overestimation at higher load levels is less pronounced. In this case, the shear retention factor is scaled linearly with the total strain in the normal direction to the crack plane. With a displacement angle of $\tan(\alpha) = \Delta U_n / \Delta U_s$, the shear retention factor reaches an asymptote. The most severe overestimation of the shear stresses is observed for the aggregate size-dependent shear retention factor eq. (3). Here, the crack normal strain is used to scale the shear retention factor, resulting in an overestimation of the shear stresses at all displacement levels, exceeding the plot boundaries. The only model that does not overpredict the shear stresses is the one that adopts a damage-based shear retention factor. As expected, the $\sigma_{\mathrm{n}} - \Delta U_n$ curves follow the same softening behavior as specified by the input tensile softening relation.

3.2 Rotating crack formulation

The same plots are generated for the rotating crack models in fig. 4b. Due to the rotation of the crack plane, the response is significantly different from the fixed crack models. Although no shear stresses exist on the rotating crack plane, the global shear stresses are considerably higher than those in the fixed crack models. Evidently, the crack plane is allowed to rotate, where the referred stresses are presented in the global coordinate system. Due to the rotation of the crack plane, in combination with the boundary condition that prohibits any horizontal strain $\varepsilon_{\mathrm{xx}}$ to develop, a significant amount of inclined compressive stress is allowed to build up due to the co-rotational formulation. This build-up of inclined and vertical stress is completely absent in the fixed crack models, where the explicit shear retention along the fixed horizontal crack controls the outcome. This behavior can also be observed in the $\sigma_{\mathrm{n}} - \Delta U_n$ curves, where compressive stresses are present in the post-softening stage. The increase in shear and compressive stresses are eventually limited by the crushing of the concrete. With the adoption of the reduction of compressive strength due to lateral cracking, the compressive strength is reduced with increasing crack strain according to eq. (4), as observed in the plots, but still the overall shear stress and normal stress are too high compared to the experiment.

3.3 Hybrid rotating-to-fixed crack formulation

The rotating-to-fixed crack results are plotted in fig. 4c For convenience, for comparing the various smeared crack models, also the fixed and rotating crack results have been added in fig. 4c. The models with transition points $\alpha_{\mathrm{fix}} = 0.7$ and $\alpha_{\mathrm{fix}} = 0.5$ do not deviate from the fixed crack formulation. As mentioned in the previous section, fixation of the crack orientation occurs before the mixed-mode loading state is reached. Conversely, the models with a transition point $\alpha_{\mathrm{fix}} = 0.0$ produce results identical to the rotating crack formulation. The rotating-to-fixed crack model with a transition point $\alpha_{\mathrm{fix}} = 0.3$ shows a transition from the rotating to the fixed crack results.

The shear stresses in the rotating-to-fixed crack model are significantly higher than those in the fixed crack formulation but lower than those in the rotating crack formulation. Similarly, the verical normal stresses are lower than those in the rotating crack formulation but higher than those in the fixed crack formulation. The $\sigma_{\mathrm{n}} - \Delta U_n$ curves exhibit the same behavior as the rotating crack formulation.

3.4 Crack dilatancy models

The results from the discrete crack dilatancy models are compared in fig. 4d. The first notable observation in the $\tau - \Delta U_n$ plots is the sudden jump in shear stress, caused by the discontinuity in the crack dilatancy stiffness matrix formulation. Up to the point where the ultimate crack strain is reached, no shear stiffness is considered. A comparison between the adopted crack dilatancy formulations indicates very similar results. However, the general trend shows that the crack dilatancy models consistently overshoot both shear and nor-

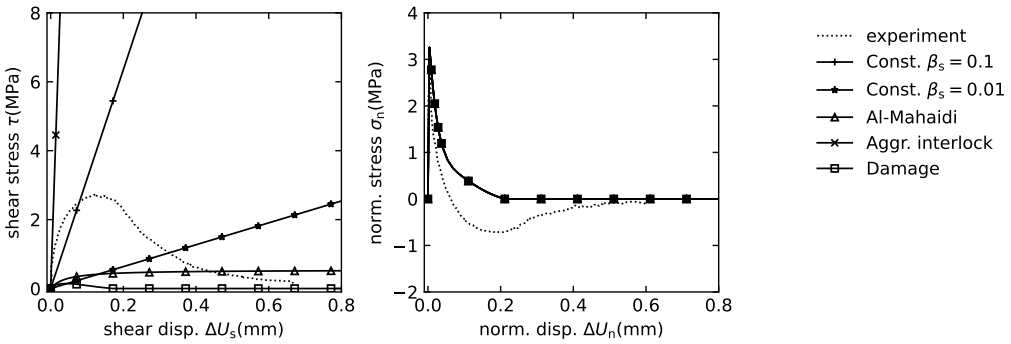

(a) Results for fixed crack formulation

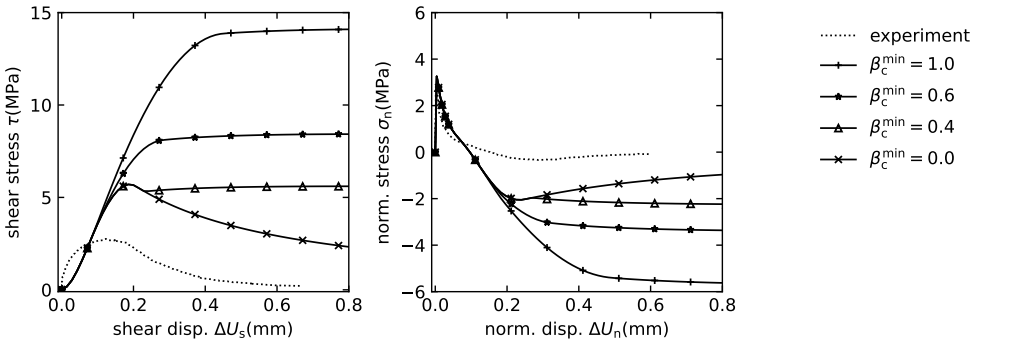

(b) Results for rotating crack formulation

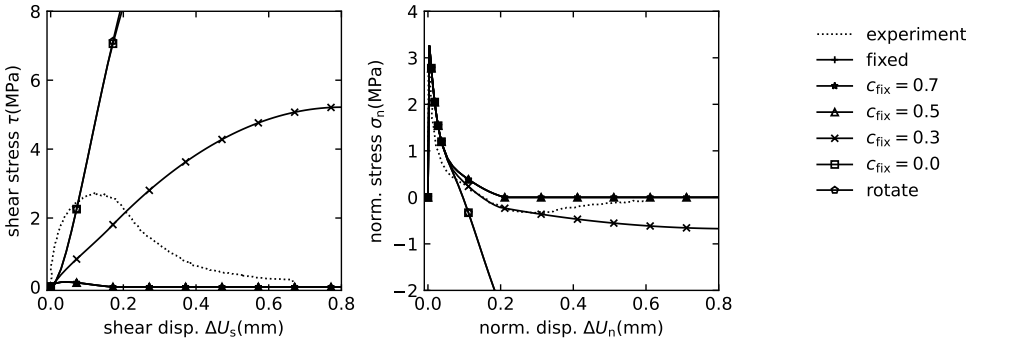

(c) Results for hybrid rotating-to-fixed crack formulation

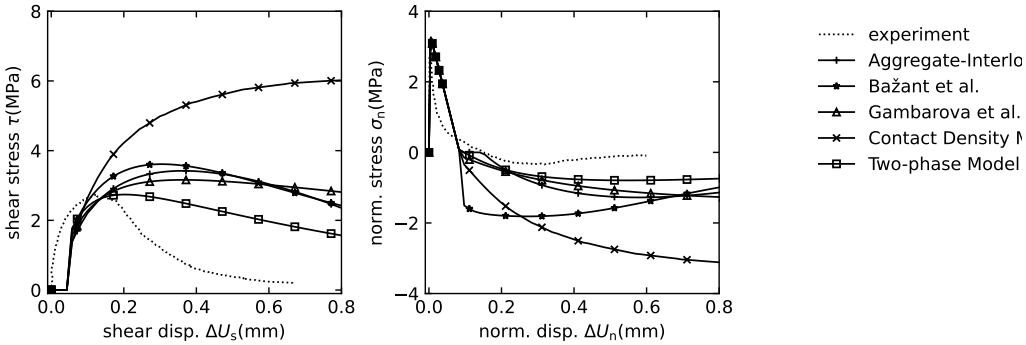

(d) Results for crack dilatancy models

Figure 4: Nominal stress-displacement response for different crack formulations; Shear component τ-ΔU_s (left) and Normal σ_{n}-ΔU_n (right) component

mal stresses to some extent, compared to the experimental results. However, compared to the smeared crack models, the crack dilatancy models exhibit more realistic behavior in terms of maximum shear stresses. In particular, the Two-phase model produces accurate results. With increasing displacements, the deviation between the numerical and experimental results increases.

4 DISCUSSION

The total strain-based crack model is known for its robustness and its conceptual simplicity with direct engineering stress-strain relations, without compromising the ability to simulate the complex behavior of concrete at a structural level. However, the results indicate that for this specific strain-driven tension-shear experiment with the specific boundary conditions of fig. 2, the fixed crack format fails to accurately capture the shear resistance. Depending on the definition of the shear retention factor, significant underpredictions or overpredictions are observed. Enhancing the model with a crack dilatancy principle could improve the results, as seen in the discrete crack approach. However, incorporating a crack dilatancy model makes the stiffness matrix non-symmetric, which is complicating the procedure, potentially compromising its robustness and deviating from the initial conceptual simplicity principle of the total strain-based crack model. An improvement in the fixed crack formulation can be achieved by refining the shear retention factor. Preliminary analysis suggests that an exponential decay of the shear retention factor as a function of the crack width would be a suitable approach and a follow-up study on this (old) topic is currently under preparation by the authors.

A notable observation in the results for the specific problem considered is the significant overprediction of shear resistance by the rotating crack formulation. The rotating crack formulation appears to produce inclined compressive stress build up for the particular boundary conditions considered ($\varepsilon_{xx} = 0$). By the introduction of the imposed shear strain, the crack plane is allowed to rotate, leading to a significant increase in the principal compressive stresses parallel to the rotating crack plane. The global shear resistance is implicitly determined by the stresses in the principal axes, in this case dominated by the formation of a compressive strut parallel to the rotating crack plane. This raises the question of whether the fully constrained boundary conditions, as prescribed in the single element test, are appropriate and representative for real strain paths that integration points undergo in real RC structures. The initial assumption was that the horizontal strain (ε_{xx}) was confined to zero, fig. 2 However, as an alternative elastic horizontal strain can be assumed to be possible. To investigate the effect, the single element test is repeated with modified boundary conditions, as shown in fig. 5. Now, the right side of the element is placed on rollers, the horizontal strain is not prescribed but free to develop, while the vertical strain and the shear strain are again prescribed as before. The results of this test are shown in fig. 6. With the adjusted boundary conditions, the shear resistance is significantly reduced and is now similar to the fixed crack model with a damage-based shear retention factor.

In the rotating-to-fixed crack formulation, the effectiveness is determined by the threshold values where the transition from a rotating to a fixed format occurs. In the analyzed benchmark problem, the rotating-to-fixed crack model generally behaves similarly to either the rotating or fixed format. In the single instance where the rotating-to-fixed model is active, no significant improvement in response is observed. Several factors contribute to this observation. Firstly, a damage-based shear retention factor is adopted once the crack direction is fixed. As found in the fixed crack formulation, this approach underestimates the shear resistance. Alternative shear retention factors could affect the response. Secondly, the transition from a rotating to a fixed crack format is based on the normal crack strain. It remains unclear if the adopted threshold value is the most suitable approach. Lastly, in experiments with different initial dis-

placements U_{n0} and mixed mode angle α, the rotating-to-fixed crack model may exhibit different behavior. Although the rotating-to-fixed crack model has the potential to improve analysis stability by reducing the stress locking effect, further investigation is required to determine its effectiveness.

The discrete crack model offers a more precise representation of shear resistance compared to smeared crack models, closer aligning with experimental observations of shear and normal stresses. However, it tends to overestimate the aggregate interlock effect, especially at larger crack widths. Despite the enhanced accuracy, the discrete crack model is impractical for full-scale structural analysis. It is more suitable when the crack location is predefined, such as at concrete-to-concrete interfaces between precast elements and cast-in-place concrete. The adopted crack dilatancy constitutive model distinguishes between the Mode I crack formation stage and the Mode II crack sliding stage, leading to a discontinuity in the shear stress-strain relationship. Further research into smoothening this discontinuity would be helpful.

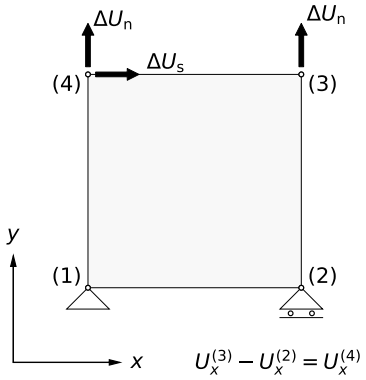

Figure 5: Smeared crack with adjusted boundary conditions

It is also worth mentioning that in the experiments, a secondary inclined crack was reported due to the aggregate interlock effect. The rotating crack formulation seems capable of capturing the formation of this secondary crack by allowing the crack to rotate. However, it does not yield accurate results for both fully constrained and unconstrained elements. From this perspective, a multi-directional crack formulation could be a more suitable approach. For now, we leave this for open discussion and will investigate it further in future research. Another discussion concerns the level of detail in the fracture process described by the adopted single element test. It is crucial to consider to what extent the chosen homogeneously strain-driven single element case can accurately represent the fracture process in the true full specimen structure. The authors acknowledge the possibility of modeling the experiment with a refined mesh. In that way, a more detailed description of the fracture process, including the formation of secondary inclined cracks, could be obtained. However, the aspects of different strain paths occurring at local integration point levels in a global structural analysis, and the marked differences between the various smeared crack approaches in that, remain as a fundamental issue as noted long before by Willam et al. [6]. As a final note, the authors would like to mention that analysis with variations in normal strain ratio's ($\varepsilon_{xx} : \varepsilon_{yy}$) as well as alternative modelling approaches, including a three-element and element assembly model, have been explored. A discussion of these results goes beyond the scope of this paper and will be addressed in a future publication.

5 CONCLUSIONS

The main focus of this study was to examine the performance of fixed, rotating and hybrid rotating-to-fixed smeared crack formulations for strain-driven elementary tension-shear model problems complying with recent mixed-mode fracture lab tests. Additionally, a discrete crack model including crack dilatancy was used for comparison. The main conclusions are:

- The shear retention factor plays a crucial role in the fixed crack results, in line with previous research. For the specific boundary conditions and strain path adopted, the models fail to capture the mixed-mode fracture behavior accurately.

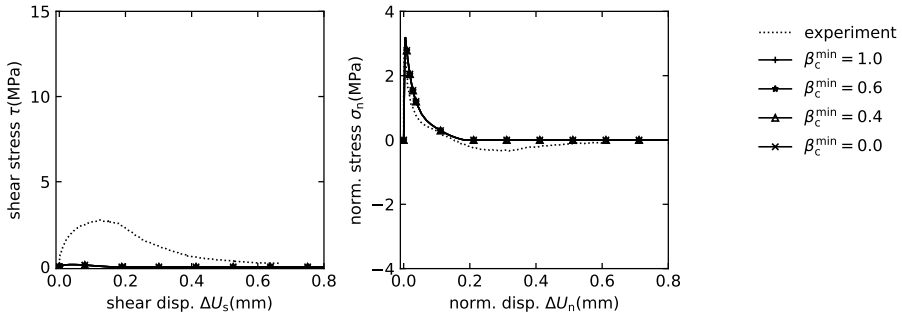

Figure 6: Nominal stress-displacement response rotating format with adjusted boundary conditions; Shear τ-ΔU_s (left) and Normal σ_{n}-ΔU_n (right) components

- The rotating crack formulation unexpectedly produced over stiff and over strong results, which was explained from the specific boundary conditions and strain path, promoting the development of a rotating compressive strut parallel to the rotating crack.

- The hybrid crack formulation does not provide any additional benefits for the tension-shear problems considered herein, and the results heavily depend on the chosen transition point for freezing of the crack directions.

- The discrete crack dilatancy models exhibit more realistic behavior compared to the smeared crack models. For the experiment under consideration, the Two-phase model produces the most accurate results.

It is almost 40 years ago that Kaspar Willam et al. [6] published their findings on fundamental issues of smeared crack models, based on a study of a specific strain-driven elementary tension-shear model problem. The present paper extends their work to different strain-paths and different boundary conditions. It demonstrates that the issues raised in [6] are still highly relevant and only partially understood, requiring further research.

6 ACKNOWLEDGEMENTS

The authors would like to thank Rijkswaterstaat for funding this research.

REFERENCES

[1] M. Hendriks, A. de Boer, and B. Belletti, "Guidelines for nonlinear finite element analysis of concrete structures," *Rijkswaterstaat Centre for Infrastructure, Report RTD*, vol. 1016, no. 1, p. 2017, 2017.

[2] P. H. Feenstra, J. G. Rots, A. Arnesen, J. G. Teigen, and K. V. Hoiseth, "A 3d constitutive model for concrete based on a co-rotational concept," 1998.

[3] N. Kostense, Y. Yang, M. Hendriks, and J. Rots, "A comparative study of implicit and explicit solution procedures for computational modeling of reinforced concrete structures," in *Proceedings of the 2024 Fracture Mechanics of Concrete and Concrete Structures Conference* (S. R. J. M. Chandra Kishen, A. Ramaswamy and R. Vidyasagar, eds.), 2023.

[4] A. de Putter, M. A. N. Hendriks, J. G. Rots, Y. Yang, M. Engen, and A. A. van den Bos, "Quantification of the resistance modeling uncertainty of 19 alternative 2d nonlinear finite element approaches benchmarked against 101 experiments on reinforced concrete beams," *Structural Concrete*, vol. 23, no. 5, pp. 2895–2909, 2022.

[5] J. G. Rots, *Computational modeling of concrete fracture*. PhD thesis, Delft University of Technology, 1988.

[6] K. Willam, E. Pramono, and S. Sture, "Fundamental issues of smeared crack models," in *Fracture of Concrete and Rock: SEM-RILEM International Conference June 17–19, 1987, Houston, Texas, USA*, pp. 142–157, Springer, 1989.

[7] J. S. Jacobsen, *Constitutive mixed mode behaviour of cracks in concrete: experimental investigations of material modelling*. PhD thesis, Department of Civil Engineering, Technical University of Denmark, Lyngby, Denmark, 2012.

[8] J. G. Rots and J. Blaauwendraad, "Crack models for concrete, discrete or smeared? fixed, multi-directional or rotating?," *HERON, 34 (1), 1989*, 1989.

[9] P. H. Feenstra, R. de Borst, and J. G. Rots, "A comparison of different crack models applied to plain and reinforced concrete," in *Proc., Int. RILEM/ESIS Conf. on Fracture Processes in Concrete, Rock and Ceramics*, (Noordwijk, Netherlands), E. and F.N. Spon, 1991.

[10] Z. P. Bažant and B. H. Oh, "Crack band theory for fracture of concrete," *Matériaux et Construction*, vol. 16, no. 3, pp. 155–177, 1983.

[11] D. A. Hordijk, *Local approach to fatigue of concrete.* PhD thesis, Delft University of Technology, 1993.

[12] P. H. Feenstra, *Computational Aspects of Biaxial Stress in Plain and Reinforced Concrete*. PhD thesis, Delft University of Technology, 1993.

[13] F. J. Vecchio and M. P. Collins, "Compression response of cracked reinforced concrete," *Journal of structural engineering*, vol. 119, no. 12, pp. 3590–3610, 1993.

[14] S. Govindjee, G. J. Kay, and J. C. Simo, "Anisotropic modelling and numerical simulation of brittle damage in concrete," *International journal for numerical methods in engineering*, vol. 38, no. 21, pp. 3611–3633, 1995.

[15] P. H. Feenstra, "Computational aspects of biaxial stress in plain and reinforced concrete," *PhD thesis, Delft University of Technology*, 1993.

[16] L. Cedolin and S. D. Poli, "Finite element studies of shear-critical r/c beams," *Journal of the Engineering Mechanics Division*, vol. 103, no. 3, pp. 395–410, 1977.

[17] R. S. H. Al-Mahaidi, "Nonlinear finite element analysis of reinforced concrete deep members," Tech. Rep. 79-1, Department of Structural Engineering, Cornell University, Ithaca, New York, 1979.

[18] M. Jirasek and T. Zimmermann, "Rotating crack model with transition to scalar damage," *Journal of Engineering Mechanics*, vol. 124, no. 3, pp. 277–284, 1998.

[19] J. Červenka, V. Červenka, U. Skandis, and L. Řehounek, "Uncertainty in the simulation of concrete fracture and comparison with blind competitions," in *11th International Conference on Fracture Mechanics of Concrete and Concrete Structures, proceedings FraMCoS-11 conf.* (S. R. J. M. Chandra Kishen, A. Ramaswamy and R. Vidyasagar, eds.), 2023.

[20] L. Østergaard, J. F. Olesen, and P. N. Poulsen, "Biaxial testing machine for mixed mode cracking of concrete," in *Fracture mechanics of concrete and concrete structures: new trends in fracture mechanics of concretes*, 2007.

[21] P. H. Feenstra, R. de Borst, and J. G. Rots, "A numerical study on crack dilatancy. part 1: Models and stability analysis," *Journal of Engineering Mechanics, ASCE*, vol. 117, no. 4, pp. 733–753, 1991.

[22] P. H. Feenstra, R. de Borst, and J. G. Rots, "A numerical study on crack dilatancy. ii: Applications," *Journal of Engi-*

neering Mechanics, ASCE, vol. 117, no. 4, pp. 754–769, 1991.

[23] Z. P. Bažant and P. G. Gambarova, "Rough crack models in reinforced concrete," *Journal of Structural Engineering, ASCE*, vol. 106, no. 4, pp. 819–842, 1980.

[24] P. G. Gambarova and C. Karakoç, "A new approach to the analysis of the confinement role in regularly cracking concrete elements," in *Proceedings of the 7th Structural Mechanics in Reactor Technology*, vol. H, pp. 251–261, 1983.

[25] J. C. Walraven and H. W. Reinhardt, "Theory and experiments on the mechanical behaviour of cracks in plain and reinforced concrete subjected to shear loading," *Heron*, vol. 26, no. 1(a), pp. 5–68, 1981.

[26] J. C. Walraven, *Aggregate interlock: a theoretical and experimental analysis*. PhD thesis, Delft University of Technology, 1980.

[27] N. Li, K. Maekawa, and H. Okamura, "Contact density model for stress transfer across cracks in concrete," *Journal of the Faculty of Engineering, University of Tokyo*, vol. XL, no. 1, pp. 9–52, 1989.